Chapter 11

GIS-Based Models as Tools for Environmental Issues: Applications in the South of Portugal

Jorge M. G. P. Isidoro, Helena M. N. P. V. Fernandez, Fernando M. G. Martins and João L. M. P. de Lima

Additional information is available at the end of the chapter

http://dx.doi.org/10.5772/48218

1. Introduction

Geographical Information Systems (GIS) simulate a given geographic space in a computational environment, allowing to store, map and analyse large amounts of georeferenced data (*e.g.*, Umbelino *et al.*, 2009). GIS were converted into a powerful tool in regional natural resources assessment, as it permits a speedy integration and representation of several biophysical attributes (*e.g.*, Bastian, 2000; Bocco *et al.*, 2001) from diverse origins such as, *e.g.*, topographic, cartographic, photogrametric, GPS and remote sensing.

The integration of Digital Terrain Models (DTM) in GIS leads to the emergence of methodologies to represent and simulate the real-word, complementing the use of thematic environmental information (*e.g.*, Felicísimo, 1999). A DTM is a numerical representation of a variable obtained from a discrete set of points, with well-known cartographic coordinates, which distribution allows calculating, by interpolation, that variable for any arbitrary point (Fernandez, 2004). If the mesh of points is altitude-related, the DTM is designated as a Digital Elevation Model (DEM). From a DEM, it becomes easy to attain topographic-derivate models (*e.g.*, slopes, orientations, curvature and visibility, shadowed and exposed areas).

Many authors have used DEM processing techniques to automatically extract geographic features (*e.g.*, Herrington & Pellegrini, 2000; MacMillan *et al.*, 2000; Burrough *et al.*, 2001; Jordán *et al.*, 2007b; Zavala *et al.*, 2005a, 2007), hydrologic structures (*e.g.*, Flanagan *et al.*, 2000; Maidment, 2000), erosive processes (*e.g.*, Zavala *et al.*, 2005b), vegetation habitats (*e.g.*, Anaya-Romero, 2004; Anaya-Romero *et al.*, 2005; Jordán *et al.*, 2007a; Pino *et al.*, 2010), among other uses.

In this chapter three GIS-based models were used, relying on different methodologies and techniques, to illustrate visualization and quantification of the geomorphic processes. This valuable input for decision-makers is attained through the versatility of GIS. Geo-form mapping in a coastal lagoon catchment, rainfall erosivity on a mountain ridge and urban flood delimitation show the potential usefulness of DEM/DTM based cartographic models for helping to solve environmental issues. All case studies presented are from the south of mainland Portugal.

The first case study is used to illustrate the main geo-form classes of the catchment including the Ria Formosa. The Ria Formosa is a shallow coastal lagoon covering an area of about 16,000 ha in the south of Portugal. It is protected by EU and national Laws, and is classified as a Wetland of International Importance under the RAMSAR convention (PORTUGAL Ramsar Site 212). This study aims to establish a method based on the Hammond hierarchical criteria and geographical information related to soft-slopes, local topography and terrain profiles, to locate and classify the geo-forms present in the Ria Formosa catchment.

The second case study focuses on the use of DEM/DTM based on climate models to obtain and analyze isohyetal maps, and to identify how rainfall distribution influences water erosion. Rainfall distribution, which is highly variable in space and time, is difficult to study, due to the lack of good quality data (*e.g.*, insufficient or poorly-distributed gauges in the study areas; non-homogeneous rainfall data series; dubious readings from non-automated gauges; lack of radar coverage). This issue may be partially addressed by geographic models (*e.g.*, DEM/DTM) and climate data related to rainfall. Parameters such as curvature, slope and orientation of hillslopes, which influence local climate, can also be obtained from these geographic models. Isohyetal maps, through multilinear regression analysis, can then be created using the DEM/DTM and their derivative models, the hillshading potential and some specific data (*e.g.* distance to coastline). From these elements and using the Modified Fournier Index (MFI), rainfall erosivity can finally be quantified. This technique was used to assess the soil erosion risks in Serra de Grândola, which is a north-south oriented mountain ridge with an altitude of 383 m, located in southwest mainland Portugal.

The third case study demonstrates the use of cartographic information to produce flood delimitation maps. The city of Tavira (10,600 inhabitants) in the south of Portugal embraces the outfall of the Séqua/Gilão River into the Atlantic Ocean. A GIS-based hydrologic model of the 221 km^2 Séqua/Gilão river catchment was first created to obtain soil use and type regional parameters. Afterwards, and to identify the maximum water heights for those return periods, a hydraulic model of the rivers' last 9.5 km was produced. These maximum water heights were compared with the observed values (flood level marks, photographs and video records) of the 3rd December 1989 flood and used to validate the model. Mean sea level changes due to climate change were also considered. With this procedure, it was finally possible to produce flood delimitation maps for the Tavira urban area. This type of modelling may provide a useful tool for urban planners and city authorities.

2. Location and classification of geo-forms in the Ria Formosa estuary

2.1. Introduction

The study of the risk of soil degradation is the starting point for development and sustainable land management. The global warming and the land use changes expected in the XXI Century predict loss of quality and reduction of soil's productivity (Cerdan *et al.*, 2010). In the Mediterranean area the natural and semi-natural vegetation is sclerophyllous, which is well suited for the local climatic conditions, however, extreme weather and human activity can cause imbalances in the ecosystem (Kosmas *et al.*, 2000). The southern Portugal is a region where the balance between the natural environment and human activity is very sensitive to erosion and desertification (Gonçalves *et al.*, 2010). Thus, it is necessary to employ control, prevention and correction measures to preserve the soil and prevent the emergence and intensification of desertification processes, which can become irreversible, as has happened in other Mediterranean areas (Kosmas *et al.*, 2000).

This study emphasizes geomorphologic processes, because they describe the natural space, the dynamics of occupations and the anthropogenic changes. According to Hammond (1954, 1964), geomorphologic studies of the earth's surface can be carried out over large areas (small scale) and based on the analysis of the land features, topographic maps or directly through field measurements. The variables considered should be quantitative, been used for a hierarchical classification.

Later, with the appearance of the GIS, Dikau (1989) and Dikau *et al.* (1991), the Hammond procedures were rectified and automated in some regions in the United States. The DEM becomes the most important tool in the process of identifying landforms. Using the "moving-window" process and through algorithms based on local operators (spatial filters) it is possible to create models (such as slope, local relief and relative position). This allows a more detailed study, with a large number of variables in a large scale. The landforms hierarchy is made in terms of size, order and geometric complexity.

Many researchers have used this methodology, although with some modifications as explained by Martínez-Zavala *et al.* (2004) and Jordan *et al.* (2005), in studies conducted in Spain and Mexico in a detailed scale. Drãgut and Blaschke (2006), and Gerçek *et al.* (2011) classified the landforms in regions of Transylvania (Romania), Germany and Turkey, respectively based in decision rules of fuzzy logic. Another technique widely used was the non-supervised classification based on levels of information. For example, Sallun *et al.* (2007) in the catchment of Alto Rio Paraná in Brazil extracted information by applying the Principal Component Analysis (PCA) in multispectral satellite images. Oliveira and Santos (2009), applied spatial filters of high pass and low pass in DEM in Feira de Santana (state of Bahia, Brazil). Teng *et al.* (2009) extracted the landforms in Shaanxi Province (China) with hillslope units from DEM.

In the present study we intend to carry out the mapping of landforms in the catchment of the Ria Formosa located in the south of Portugal (Algarve), using the methodology followed by Jordán *et al.* (2005), modified in order to take in consideration the specific features of this region.

This study contributes to a better characterization of the region allowing the preparation of regional plans to control the processes of soil degradation, with an indication of possible uses and restrictions.

2.2. Study area

The Ria Formosa catchment is limited by the WGS84 coordinates 37º 15′ N to 36º 57′ N and 7º 28′ W to 8º 4′ W. It has an area of 864 km² and a perimeter of 166 km, including a shallow coastal lagoon with an area of about 16,000 ha. It is protected by EU and Portuguese Laws, and is classified as a Wetland of International Importance under the RAMSAR convention (PORTUGAL Ramsar Site 212). It covers the municipal areas of Tavira, Faro, Olhão, São Brás, Loulé, Vila Real de Santo António and Castro Marim. The topography of the region is regular and continuous without abrupt changes in altitude. The average slope is 11% and the elevation varies between 0 and 530 meters above sea level. Mean annual rainfall of the catchment ranges between 400 and 800 mm. The mean annual temperature is 17 ° C.

2.3. Methodology

The DEM has been used as a basic source of information on the catchment of the Ria Formosa and was obtained from a geostatistical study with a resolution of 10×10 m², which was based on cartography at the scale 1:25,000 from the Geographical Institute of the Portuguese Army (IGeoE, 2004). From this model, other information about other terrain features were obtained. The analysis and mapping of the data has been performed with the IDRISI Taiga software (Eastman, 2009). With this software, several terrain variables such as slope, curvature, relative position, and local relief were modelled for each point relatively to the DEM. Finally, the automatic classification of landforms was carried out, as established by Jordan *et al.* (2005).

2.3.1. Slope and curvature

Maps of slopes and curvatures are commonly used to describe the hydrologic drainage structure of a region or a catchment. Soil properties and the characteristics of the hillslopes are factors that combined determinate a higher or lower resistance to soil erosion, especially due to rainfall. The inclination, the length and the shape of a slope are associated to the velocity of runoff and to the water infiltration into the soil.

The slope at point (*M*, *P*), in the azimuth direction *A*, is given by calculating the inner product between the gradient of the surface *H* and the unit vector $\vec{w}_A$ with the components ($\alpha = SinA$; $\beta = CosA$):

$$\nabla H \mid \vec{w}_A = \frac{\partial H}{\partial X}\alpha + \frac{\partial H}{\partial Y}\beta = \left\|\nabla H\right\| = \sqrt{\left(\frac{\partial H}{\partial X}\right)^2 + \left(\frac{\partial H}{\partial Y}\right)^2} \quad (1)$$

When the ground is represented by a matrix *H* (m, n), *X* and *Y* are coordinate axes, and the gradient of the surface *H* represents the topography of a square that includes point (*M*,*P*) defined by a bi-linear polynomial expression:

$$H = aMP + bM + cP + d \tag{2}$$

The coefficients *a*, *b*, *c* and *d* are determined at the expense of the coordinates of the square-defined four vertices.

The determining of slope of each pixel in line l and column *k* is based on elevation values of neighbouring pixels and the spatial resolution of the model, *E* (distance between pixels). The slope is calculated using Eq. (3).

$$\delta = \sqrt{\left(\frac{H(l,k+1) - H(l,k-1)}{2E}\right)^2 + \left(\frac{H(l-1,k) - H(l+1,k)}{2E}\right)^2} \tag{3}$$

From the analysis a smooth slope map was produced, using the "Moving Window" technique with a size of 4,900 m² (*i.e.*, 7×7 matrix). For each window was determined a percentage of soft slope (considered below 4%), and that value was assigned to the central pixel of the window. After this process, the map was reclassified (Table 1).

Code	Percentage of soft slope
1	More than 80%
2	50% at 80%
3	20% at 50%
4	Less than 20%

Table 1. Reclassification of the slopes by percentage of soft slopes.

The curvature is defined according to the rate of change of the slope, which is determined by the partial derivatives of second degree of surface *H*:

$$C_A = \nabla^2 H = \frac{\partial^2 H}{\partial X^2} + \frac{\partial^2 H}{\partial Y^2} \tag{4}$$

As we are working on a discrete space, it is possible to approximate the Laplacian in two dimensions, using the finite difference method, being the size equal to the unity (one cell):

$$\nabla^2 H = H(l+1,k) + H(l-1,k) + H(l,k+1) + H(l,k-1) - 4H(l,k) \tag{5}$$

Therefore, the same expression in the matrix form, can be written as follows:

$$\begin{bmatrix} 0 & 1 & 0 \\ 1 & -4 & 1 \\ 0 & 1 & 0 \end{bmatrix} \tag{6}$$

This matrix 3×3 is called the Laplacian filter, which was used in a spatial convolution process on the MDT, wherein each central cell of the window was assigned a curvature value. The negative values indicate concavity (sedimentation basins, valleys, etc.), while

positive values indicate convexity (massifs, domes, peaks, upper parts of slopes, etc.). The values equal or very close to zero correspond to flat surfaces.

After extraction of the curvature, it was necessary to make a spatial convolution in order to filter the unhelpful and inconsistent information and highlight the most important formations. We used a Gaussian filter with 10×10 m^2 cells within a 7×7 matrix.

2.3.2. Local relief and relative position

The local relief can be expressed as the vertical difference between the highest point and the lowest points, of a surface, within a certain horizontal distance or in a determined area of analysis (Figure 1; Left). The relative position sets up the flat shapes of the terrain, in uplands and lowlands, separating the plateaus from the plains with hills or mountains. In this study we considered that all concave and convex areas were, respectively, lowlands and highlands (Figure 1; Right).

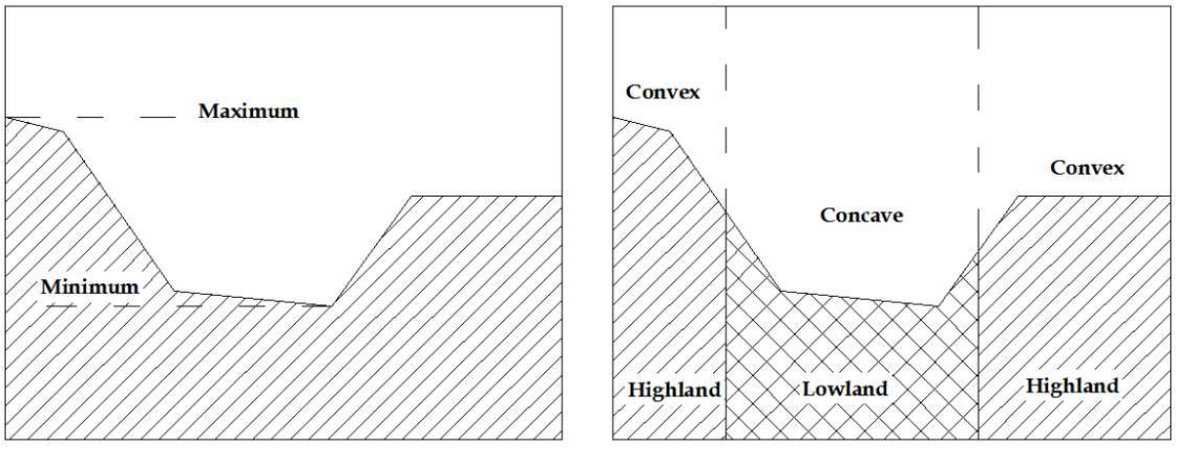

Figure 1. Left: Local relief; Right: Relative position.

The determination of the local relief was calculated directly from the MDE, through two spatial convolution processes of a (7×7) matrix. The maximum and minimum elevations were determined and replaced in the respective central cells. At the end the results were subtracted. After this process, the map was reclassified as follows (Table 2).

Code	Class	Classification
1	0 - 15 m	Very smooth
2	15 - 30 m	Smooth
3	30 - 90 m	Localized
4	90 - 150 m	Moderate
5	150 - 220 m	Rough

Table 2. Classes of the local relief.

To calculate the relative position, the curvature and the smooth slopes (<4%) were integrated. The classification was used to define the classes presented in Table 3.

Code	Class
a	> 75% of smooth slopes on concaves hillsides
b	50 – 75 % of smooth slopes on concaves hillsides
c	50 – 75 % of smooth slopes on convexes hillsides
d	> 75% of smooth slopes on convexes hillsides

Table 3. Classes of the relative position.

2.3.3. Landforms

The mapping of landforms was constructed by crossing three levels of information: smooth slope, local relief and relative position. The five main forms considered were: plains, plateaus, plains with hills, and open hills. In turn, these classes were divided into twenty sub-classes.

2.4. Results and discussion

The main forms and the respective subclasses, for the region of Ria Formosa are shown in Figure 2 and Table 4.

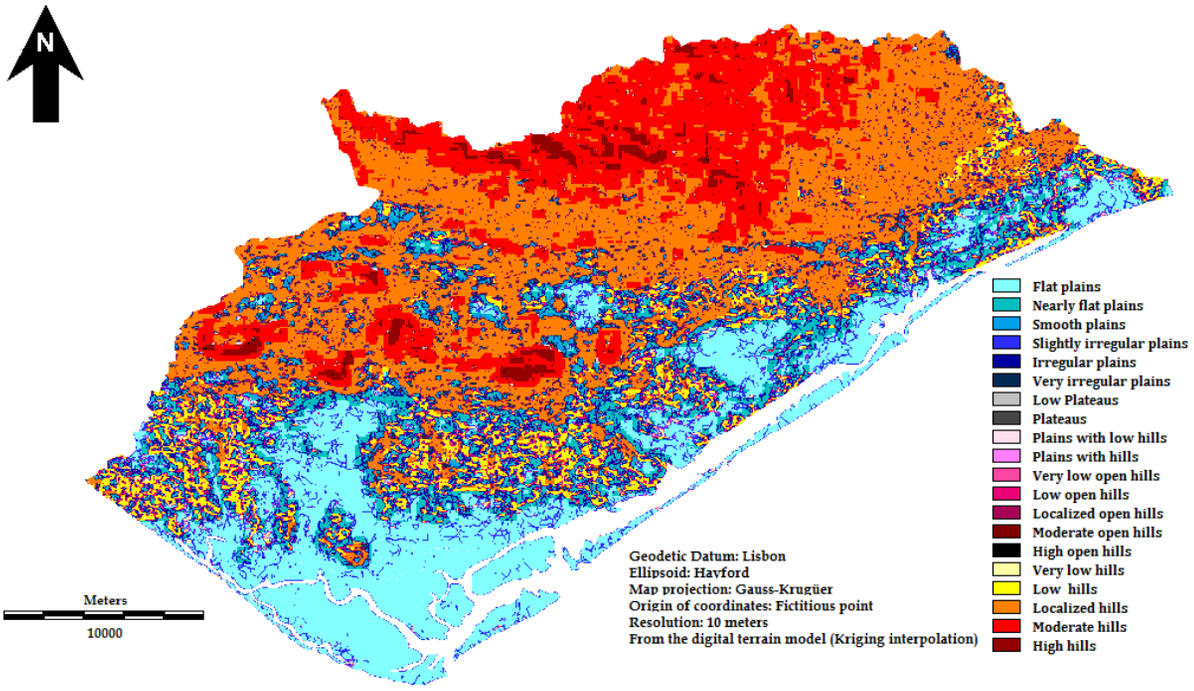

Figure 2. Map of landforms in the Ria Formosa catchment.

As can be seen, the *localized hills* and *moderate hills* (Table 4) cover most of the catchment area (43%), mainly on areas such as Mountain of Caldeirão, and the mountain formations of carbonated rocks (Monte Figo, Malhão, Guilhim and Nexe).

In particular, in the Mountain of Caldeirão, there is a very dense drainage network due to the formation of Flysch from Baixo Alentejo region, consisting of turbidites (greywackes,

silts and shales) which, because of its layered structure, hamper the infiltration of surface runoff. On the other hand the vegetation is typically mediterranean, composed by quercíneas and sclerophyllous over Eutric Leptosol. Therefore on more rugged slopes, there is little capacity for water storage, making it difficult to sustain the vegetation. Furthermore, poor agricultural practices have been destroying the natural vegetation, causing in the rainy season a deterioration of these soils and turning them into skeletal. So the predictable risk of erosion ranges from moderate to high.

The flat plains are the second class of the highest representation (25.3%), distributed on the littoral, next to the Ria Formosa and along the leeward coast. These flat surfaces, with less dense dendritic drainage systems, are composed mainly of alluvium, sand dunes and pebbles (slightly cohesive soils and sediments). This system flows in parallel form to the arms of the estuary and may be subject to flooding. These areas are fluvisol, luvisols and cambisols and are fertile for agriculture. They have dense vegetation, with orchards and complex cultural systems providing a low or moderate risk of soil erosion.

Class	Subclass	Code	Area (km^2)
Plains	Flat plains	11a 11b 11c 11d	142.93
	Nearly flat plains	12a 12b 12c 12d	65.92
	Smooth plains	13a 13b 13c 13d	16.04
	Slightly irregular plains	21a 21b 21c 21d	27.51
	Irregular plains	22a 22b 22c 22d	52.62
	Very irregular plains	23a 23b 23c 23d	23.97
Plateaus	Low Plateaus	14c 14d 24c 24d	0.52
	Plateaus	15c 15d 25c 25d	0.02
Plains with hills	Plains with low hills	14a 14b 24a 24b	0.63
	Plains with hills	15a 15b 25a 25b	0.01
Open hills	Very low open hills	31a 31b 31c 31d	3.84
	Low open hills	32a 32b 32c 32d	32.33
	Localized open hills	33a 33b 33c 33d	37.38
	Moderate open hills	34a 34b 34c 34d	3.48
	High open hills	35a 35b 35c 35d	0.13
Hills	Very low hills	41a 41b 41c 41d	2.22
	Low hills	42a 42b 42c 42d	46.44
	Localized hills	43a 43b 43c 43d	226.67
	Moderate hills	44a 44b 44c 44d	128.85
	High hills	45a 45b 45c 45d	14.45

Table 4. Classification of 20 classes of landforms and their cover area (Ria Formosa).

2.5. Conclusions

Using an automatic hierarchical method for classification the Ria Formosa drainage basin has been subdivided in twenty landforms. The area included in each class is characterized

by a number of geomorphologic characteristics, which distinguishes them from neighbouring areas. The localized and moderate hills and flat plains are the classes with the highest representation. Allied to information on soil type and vegetation cover, the former, appears to have a moderate to high erosion risk and the latter might have a low to moderate risk. However, in future research, it is intended to create a more accurate map of erosion risks, by matching the satellite images, climatic data, mapping of land use, geological and pedological features in an appropriate scale. Moreover, methodology used in this study for landform mapping, can also be validated by elaborating a descriptive mapping of a sample area, based in photo interpretation and field observations. The aerial photography, with 60% overlap, allows the creation of stereoscopic pairs which facilitate the characterization of the terrain. Fieldwork will also be useful for add and/or confirm the information obtained by stereo restitution. Comparison of the pixels in each unit of land allows validating the model.

3. Mapping of rainfall erosion in Serra de Grândola

3.1. Introduction

Erosion is a global scale threat to sustainability and productive capacity of the soil (*e.g.*, Yang *et al.*, 2003; Feng *et al.*, 2010). It is estimated that about 10 million hectares of farmland are lost annually in the world due to soil erosion (Yang *et al.*, 2003; Pimentel, 2006).

Climate change may have a great influence in soil erosion (Pruski and Nearing, 2002). Changes in the erosive power of rainfall can be hazardous in terms of soil erosion (Favis-Mortlock and Savabi, 1996; Williams *et al.*, 1996; Favis-Mortlock and Guerra, 1999; Pruski and Nearing, 2002).

Erosion, the most common type of soil degradation, should be considered as the main symptom of desertification. Since the first half of the XX Century numerous studies have been carried out and gave a strong contribution to the knowledge on the mechanical processes leading to erosion and how these processes interact in the environment. However, studies on how social, economic, political and institutional factors are affected by erosion, have been developed only during the last decades.

According to the digital Soil Map of the World (FAO, 1989) and a climate database Eswaran *et al.* (2001) the vulnerability to desertification of the Mediterranean area countries, it is considered that more than 600,000 km^2 of the Mediterranean basin are at risk of desertification. Project DesertWatch, presented at the 10th Conference of the Parties to the United Nations Convention to Combat Desertification, states that the 33% of the Portuguese territory is at risk of desertification, being the Alentejo the most affected area.

The main objective of this work is the development of a GIS to determine the risk of erosion in Serra de Grândola (Alentejo, Portugal).

3.2. Study area

The study area is delimited by the UTM coordinates: Zone 29S, M_{min}=512,930.44 m, P_{min}=4,205,893.13 m, $M_{máx}$=540,965.44 m, $P_{máx}$=4,230,328.13 m. Its area, with 675 km^2, includes

the Grândola, Sines and Santiago do Cacém municipalities, and the mountain Serra de Grândola (maximum altitude: 383 m). Serra de Grândola extends up to the West coast, in a regular and continuous form, without major abrupt changes in topography. Annual rainfall ranges from 600 to 1,200 mm. The Atlantic-influenced climate is moderate, with average annual temperatures of 17^0 C. Lithologically there are three important groups (1:50,000 Portuguese Geological Map; DGM, 1984): (i) in the highlands, the Flysch formation of the lower Alentejo, (ii) in the highlands surrounding areas, sandstones and gravel of the littoral of Lower Alentejo and Vale do Sado and, (iii) in the coastal zone, the beach and sand dunes. Pedologically there is a predominance of Eutric Lithosols (highlands) and Podzols (coastal zone).

3.3. Methodology

Based on the intersection of the soil's erosive status with the rainfall aggressivity, the latter classified according to the Modified Fournier Index (MFI), the risk of erosion at the Serra de Grândola was assessed (Figure 3) using IDRISI Taiga software (Eastman, 2009).

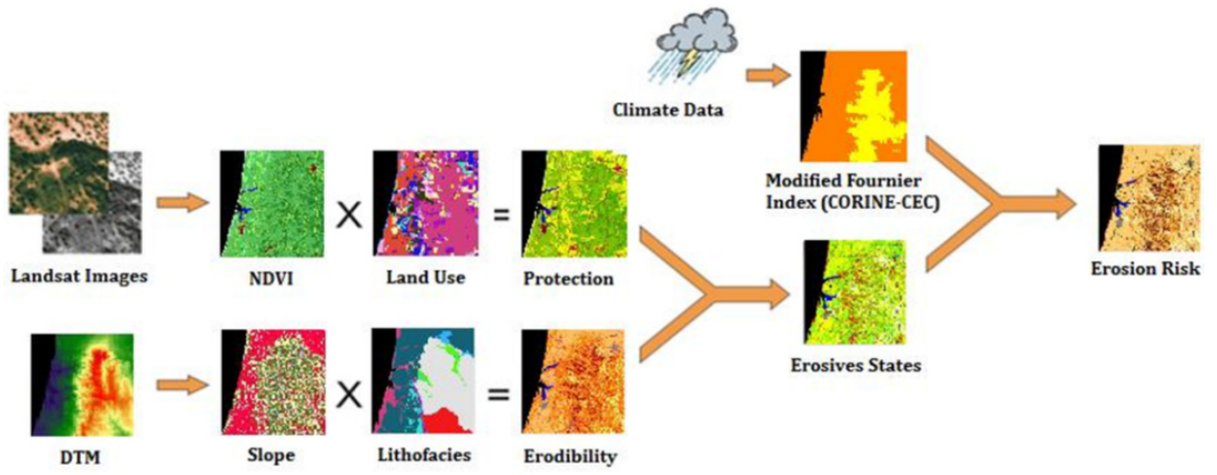

Figure 3. Schematic of the methodology used in this application.

3.3.1. Mapping of the erosive status

The vegetation coverage map was obtained by applying vegetation indexes developed in order to simplify the number of parameters present in the multi-spectral measurements. These indexes, generated from remote sensing data, constitute an important way to include anthropic activity in the ecosystems. Although there are many vegetation index available in the literature, because vegetation has a high reflectance in Near Infra-Red (NIR) and a low reflectance in R (*e.g.*, Lillesand *et al.*, 2004), this study used the Normalized Difference Vegetation Index (NDVI), a technique introduced by Rouse *et al.* (1974) which enables to know the density and the state (greenness) of the vegetation cover.

The land use information was obtained from the CORINE Land Cover map (CORINE-CLC, 2006) at a 1:100,000 scale. The map, based on satellite images SPOT-4, SPOT-5 and IRS-P6

LISS III, represents 44 classes of land use with a 150 m of positional accuracy resolution, with a minimum mapping unit of 25 ha.

The soil protection map was obtained by crossing the land use map with the vegetation coverage map. According to the classification proposed by Zavala (2001) the soil protection was classified into the following classes: 1-Very High, 2- High, 3- Moderate, 4- Low , 5- Very Low 6- Unprotected.

A DEM was obtained by ordinary kriging of 32,000 points, which were retrieved from a set of 526,770 points obtained from discretization of 10 m equidistant contour lines (military 1:25,000 map).

The hillslopes map was obtained from the DEM (see Eq.(3)). The slopes were classified into ranges: 0-3%, 3-16%, 16-21%, 21-31% and over 31%.

The lithofacies map was created from a 1:50,000 scale Portuguese Geological Map (DGM, 1984). Five lithofacies classes were defined based on the PAP/RAC, (1997) classification.

The erodibility map was obtained by crossing the slope and lithofaceis maps. Accordingly to Zavala (2001) five levels of erodibility were set: 1- Very Low, 2- Low, 3- Moderate, 4- High and 5- Very High.

The erosive status map was obtained by crossing erodibility and soil protection maps. According to Zavala (2001) five levels of erosive status were set: 1- Very Low, 2- Low, 3- Moderate, 4- High and 5- Very High. Soil erosive states are expressed in terms of protection and erodibility (Table 5).

Protection	**Erodibility**				
Classes	1	2	3	4	5
1	1	1	1	2	2
2	1	1	2	3	4
3	1	2	3	4	4
4	2	3	3	5	5
5	2	3	4	5	5
Unprotect	3	4	5	5	5

Table 5. Classification of soil erosive status.

3.3.2. Modified Fournier Index model

The Modified Fournier Index (*MFI*), an improved version of the Fournier Index (*FI*); Fournier (1960), is used to estimate the rainfall aggressivity for all months as in this area it occurs along the year, since the *FI* is only used in regions characterized by dry seasons. The *MFI* is calculated by Eq. (7) (*e.g.*, Arnouldus, 1978).

$$MFI = \sum_{i=1}^{n} \frac{P_i}{P_t}. \tag{7}$$

where: P_i is the monthly rainfall at month i (mm) and P_t is the annual rainfall (mm).

Monthly rainfall data observed from 01.01.1911 to 31.12.2010 on 30 weather stations were used as an input to the *MFI* model.

Rainfall distribution is highly variable in space and time. In this study the precipitation data are insufficient and poorly distributed. Thus, for creating the MFI model other variables which are correlated with precipitation were used such as hillshading, aspect, distance to coastline, latitude and elevation. The software Statistica 6.0 (Statsoft, 2001) was used to establish a multilinear regression with t critical=1.711 for a significance of 95% (α = 0.05). Aspect model was created based on DEM, by Eq. (8).

$$Aspect = \text{atan2}\left(\frac{dz}{dy}, -\frac{dz}{dx}\right) \tag{8}$$

where: $\frac{dz}{dy}$ is the variation of height in latitude and $\frac{dz}{dx}$ is the variation of height in longitude.

Models of hillshading created refer to solstice and equinox. These models represent the hillshading for a given solar declination and azimuth. These variables were calculated using the equations described by Díez-Herrero *et al.* (2006). Hillshading models were calculated with Eq. (9).

$$HS = 255\left[\left(Sin(\gamma)\right)Cos(D) + Cos(\gamma)Sin(D)Cos(\phi - A)\right] \tag{9}$$

where: *HS* is the hillshading, γ (º) is the elevation of the sun above the horizon, *D* (º) is the declination of the sun, ϕ (º) is the solar azimuth and *A* (º) is de aspect.

While mapping of the MFI various models were created and the respective outputs analysed such as Cook's distance, consistency, independence and normality. The best model found was that in which the independent variables were latitude, elevation, and distance to coastline, spring hillshading and aspect:

$$R = 1.1708\,E + 0.0009\,L + 708.8582\,SHS - 0.1225\,A - 0.0032\,DC - 3{,}432.4703 \tag{10}$$

where: *R* (mm) is rainfall, *E* (º) is elevation, *L* (º) is latitude, *SHS* is spring hillshading, *A* (º) is aspect and *DC* (m) is a distance to coastline.

Classes	Range	Classification
1	<60	Very low
2	60-90	Low
3	90-120	Moderate
4	120-160	High
5	>160	Very high

Table 6. *MFI* values according CORINE – CEC (1992).

3.3.3. Erosion risk mapping

Finally, the erosion risk map (Figure 4) was obtained by relating the erosive status and MFI classified according to CORINE-CEC (1992). According to Zavala (2001), five levels of erosion risk were set: 1- Very Low, 2- Low, 3- Moderate, 4- High and 5- Very High. Erosion risk was expressed in terms of erosive status and MFI (Corine-CEC, 1992) (Table 7).

Erosive status	MFI (Corine-CEC)				
	1	**2**	**3**	**4**	**5**
1	1	1	1	2	3
2	1	2	2	3	4
3	1	2	3	4	5
4	2	3	4	4	5
5	3	4	5	5	5

Table 7. Determination of the levels of erosion risk as a function of the erosive status and the rainfall aggressivity.

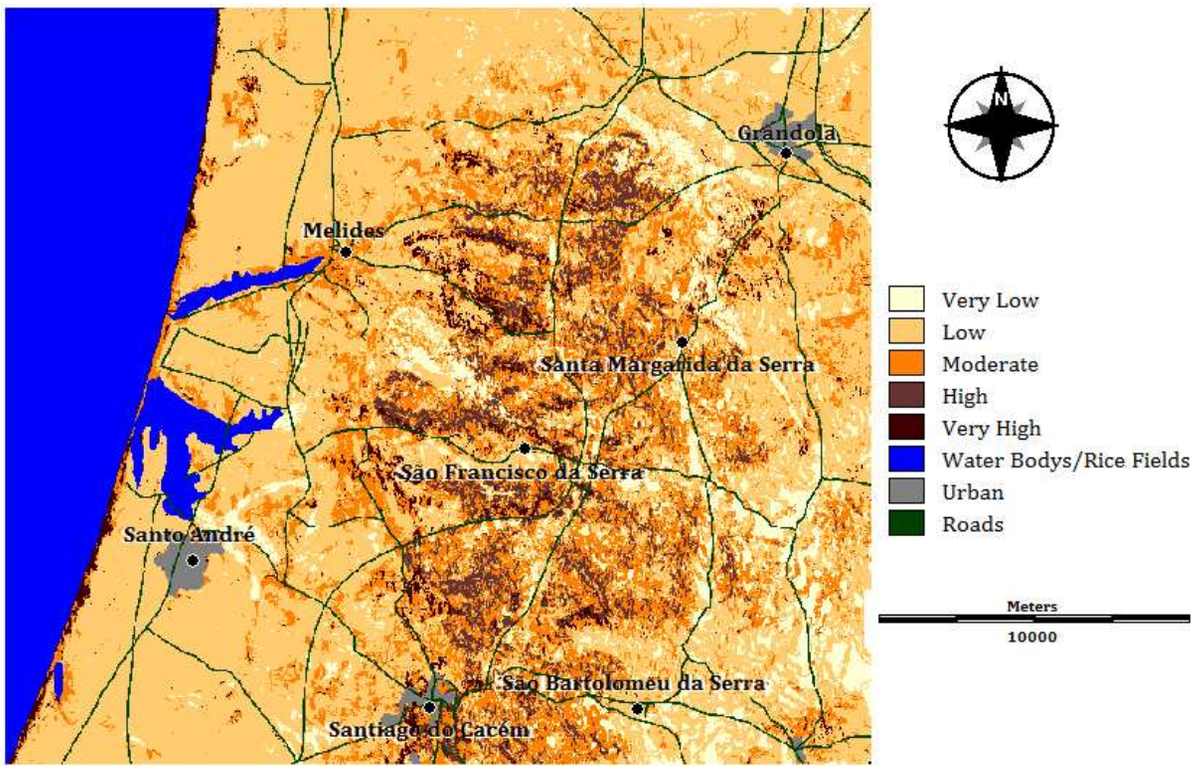

Figure 4. Digital model of the annual risk of erosion of the Serra de Grândola.

3.4. Results and discussion

3.4.1. Erosive status map

Each erosive status class was characterized according to the slope, soil and vegetation cover (Table 8).

Table 8 shows that most representative classes have low risk (28%) and moderate risk (44%) of soil erosion, usually on the highlands or at the coastal areas. The coastline consists mainly of cliffs with non-cohesive materials (sand and gravel). In the highlands the material is more resistant (Flysch group from lower Alentejo) but the amount of rainfall is higher and the steep slopes favour soil erosion processes. Soils with material from class D (soil or poorly resistant or deeply altered rocks) and E (soils or sediments that are poorly cohesive or detritus materials) are the most representative, with slopes ranging between 0-3% (slow runoff) and 3-16% (moderate runoff).

3.4.2. Modified Fournier Index

All study areas, classified according to CORINE - CEC (1992), present values of *MFI* of low risk (71%) and moderate risk (29%) of erosion, which means a small aggressiveness of rainfall.

Erosive State	Occupation	Slope	Soil	Land Cover
Very Low	10%	0-3%	Schists, phyllites, silltites, quartzites and Flysch group	Hardwood forest
			Dunes	Permanently irrigated land
Low	28%	0-3%	Sand, sandstone and gravel	Coniferous forest
		3-16%	Flysch group	Hardwood forest
Moderate	44 %	3-16%	Sand, sandstone, gravel and dunes	Coniferous forest
			Flysch group	Hardwood forest
High	16%	3-16%	Limestone, dolomite, sand, sandstone gravel and dunes	Cultures /systems fragmented complex / non-irrigated arable land
		16-31%	Flysch group	Hardwood forest/agro forestry
Very High	3%	21-31%	Limestone, dolomite, sand, sandstone gravel and dunes	Non-irrigated arable land/ forest or shrub vegetation transition/beaches
			Flysch group	Agro-forestry

Table 8. Characterization of the erosive status.

3.5. Conclusions

Environmental biophysics requires knowledge of the resources and processes affecting ecological systems conservation, as well as planning and land management. In completion of the erosion cartography it was possible to develop topographic models (slope, orientation of slopes and distance to the coastline), climate (rainfall, hillshading, Modified Fournier index) and lithofaces. These models represent quantitatively the environmental variables that affect the process of erosion.

Moderate erosive status is the most frequent class in the study area. Highlands, where the soil material have moderate resistance (flysch formation) and the precipitation is higher, and the coastline, essentially composed of cliffs with low cohesive material (sand gravel), are the most sensitive areas to erosion. However, using this erosive model it is difficult to justify the risk of water erosion at the coastline. In coastal areas infiltration prevails (sand dunes) and the wind action is the most important factor in the erosion process. Therefore, in future studies, the model should be capable of including wind erosion.

The largest amount of precipitation is falling in December and January and the lowest in July and August. Through the mapping of the rainfall erosivity, it was found that the aggressiveness of rain in the coastline and in the highlands is higher in these months.

4. Flood delimitation mapping of the Tavira urban area

4.1. Introduction and objective

This case study illustrates the use of GIS as a tool to establish hydrologic regional parameters for urban flood mapping purposes. Cartographic elements, hydrological and hydraulic models, and boundary conditions used to establish the maximum flood levels of a 10- and a 100-years return period flood and a 100-years climate change scenario are described. Cartographic information was completed by *in-situ* measurements and observations.

Hydrologic regional parameters are extensively used in flood simulation, since drainage basins are characterized by natural variability in land-surface features (*e.g.*, Wooldridge and Kalma, 2001). Prasad (1997) refers that the improved accuracy of GIS-based hydrologic simulation comes from the capability that these models have to integrate hydrologic regional parameters; updating or modifying GIS data to study the impact of changes in a drainage basin (*e.g.*, land use) becomes a relatively easy task.

This application is focused on the simulation of fluvial-originated urban flooding. The area selected for this study is the town of Tavira. This town is situated in the southernmost region of Portugal – Algarve. The Séqua/Gilão River crosses throughout the Tavira urban area until it flows into the Ria Formosa coastal lagoon. As the Séqua/Gilão River is intrinsically connected with the urban fabric, an overtopping of the margins always has negative consequences to people and assets. An example of a severe flood event was the 3rd December 1989 flood which caused extensive damage in the city.

4.2. Study area

Tavira (12,000 inhabitants) is one of the southernmost towns of mainland Portugal. The town origins come back since about 2,000 BC and from these years until the half of the last century Tavira has had in agriculture and fishing its major economical activities. Like many areas in the Algarve region, in these last decades, tourism has gained a sound importance in the local economy and lifestyle. The Séqua/Gilão River, which crosses the entire town, is crossed by 6 bridges.

This study characterizes the whole river basin of the Rio Séqua/Gilão with length of the river valley of 9.5 km from the outlet. The drainage basin of the Séqua/Gilão River considered for this study is located immediately upstream of the northern limit of Tavira's urban area (top left of Figure 5).

4.3. Materials and methods

This section presents the hydrologic and hydrodynamic models used to determine the peak flows and the delimitation of the flooded areas. Particular attention was given to obtaining the hydrologic parameters related to soil use and type (CN values; Brunner, 2006). The flood delimitation methodology and the verification of the modelled flood – by comparison with observed data – are also presented.

Figure 5. Urban area of Tavira and the Séqua Gilão River, flowing from left to right.

4.3.1. Hydrologic model

The Séqua/Gilão drainage basin has an area of 227 km² immediately upstream of Tavira. This drainage basin can be divided into 4 sub-basins, namely: Alportel, Asseca, Fornalha and Séqua (Figure 6). Characteristics of the sub-basins are shown in Table 9.

Characteristics of the drainage sub-basins and rivers	Sub-basins			
	Alportel	**Asseca**	**Fornalha**	**Séqua**
Sub-basin area (km²)	93.12	61.35	40.06	32.31
Main river length (km)	49.07	19.77	15.06	14.25
Equivalent slope (m/km)	6.5	9.4	17.6	5.9
Time of Concentration (h)	9.2	4.0	2.5	3.7
Lag-time (h)	5.5	2.4	1.5	2.2

Table 9. Major hydrological and physical characteristics of the drainage sub-basins and rivers of the Séqua/Gilão River.

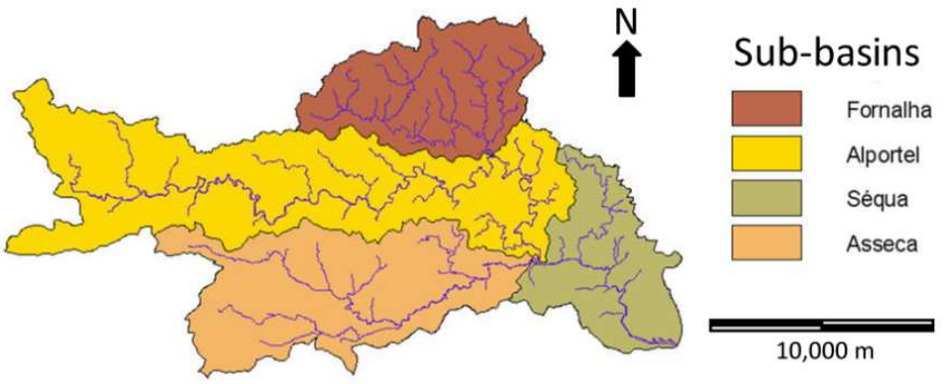

Figure 6. Drainage basin of the Séqua/Gilão River immediately upstream of Tavira. The 4 sub-basins are identified.

According to the Portuguese Soils Map (SROA, 1970) most of the soils of the Séqua/Gilão drainage basin may be classified as "Ex - Lithosols of xeric regime climate, schists or greywackes" (Cardoso, 1965). Soils properties were defined using field tests data (Koop *et al.*, 1989). The soils hydrologic groups were defined (*e.g.*, Lencastre and Franco, 1992) as B, C and D (US Soil Conservation Service Curve Number method). Group D was by far the most common in the drainage basin. Soil use was acquired via the Corine Land Cover chart and largely consists of forests and farmlands. According to the Curve Number method, information on the soil types and uses were combined to obtain the CN II values, to which soil types and uses determine the relationship between rainfall and effective rainfall for soil moisture conditions between the wilting point and field capacity. However, in flood-related studies, the soil moisture conditions should correspond to soils with high water content which are able to reach or surpass field capacity, a situation that leads to the origin of larger floods. Adjusted values (CN III) used in this study are shown in Figure 7.

The design hyetographs were obtained by using Intensity-Duration-Frequency curves referred in the Portuguese Law (DR 23/95 of 23rd August) and the "alternating block

method" (Chow, 1988). Kirpich formula (*e.g.*, Guo, 2006; de Lima, 2010) was used do estimate the Time of Concentration of each of the sub-basins; the Lag-times were approximated as 60% of the latter (Table 9).

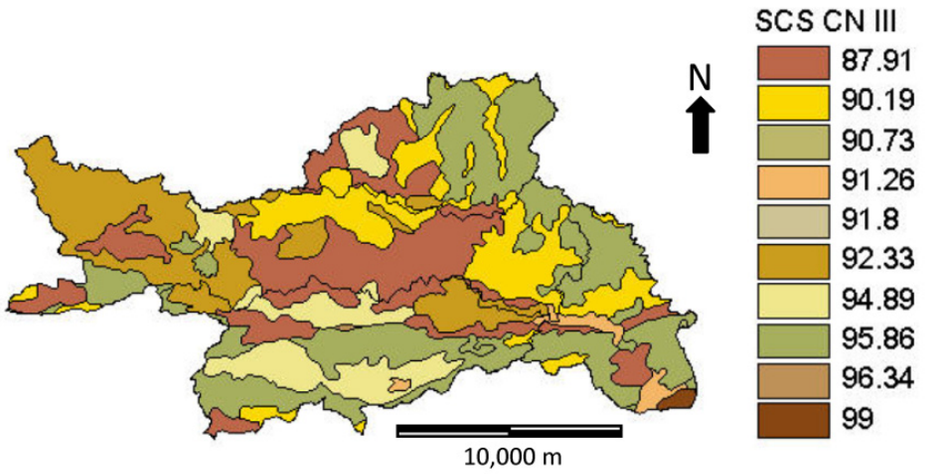

Figure 7. Soil Conservation Service CN III values for the drainage basin of the Séqua/Gilão River.

The information above served as an input to the HEC–HMS model (Brunner, 2006). Data for the drainage basin watershed were introduced into the model, differentiating the four sub-basins and their topological connections, the reaches and the final section of the drainage basin (sink). Resulting Séqua/Gilão River basin model is shown schematically (Figure 8).

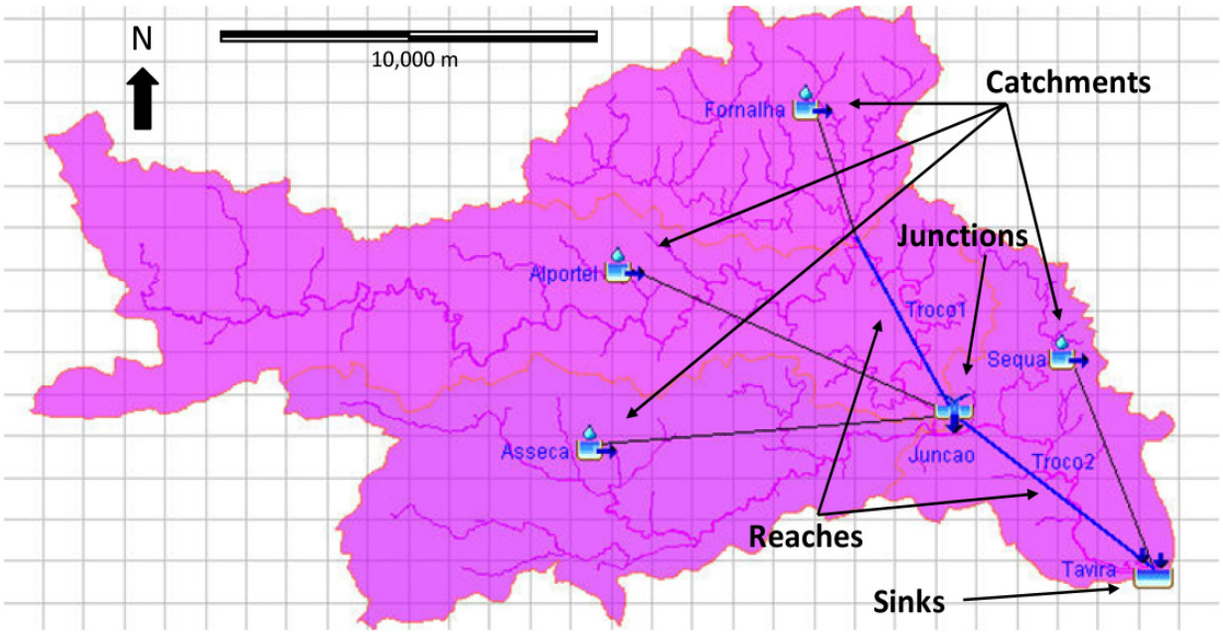

Figure 8. Topological scheme of the Séqua/Gilão River drainage basin.

The resulting design hydrographs produced peak flows for the 10- and 100-years return period, respectively, of 520.6 m^3/s and 928.0 m^3/s.

4.3.2. Hydrodynamic model

The HEC–RAS model (Hydraulic Engineering Center – River Analysis System) was used to define, for the full extension of the Séqua/Gilão River, the maximum flood levels to be expected for 10- and 100-years recurrence periods. In the simulation it was assumed (i) a 1D unsteady flow, (ii) inflow in the upstream boundary condition is defined by the previously obtained design hydrographs, (iii) water level at the downstream boundary condition is defined by expected spring tide levels at Faro bar and an additional climate change scenario with a mean sea rise of 0.91 m was also used (mean sea rise value was imposed by national authorities), (iv) flow resistance is approximated by the Manning-Strickler equation, (v) densely urbanized areas are considered as non-effective flow areas, *i.e.*, where water overflows and returns in the same river section and (iv) head loss in hydraulic structures (*e.g.*, bridges) is due both to the head loss during flow along the hydraulic structure and the localized head loss.

The main flow line was discretized by cross sections (STs) of the river, based in topographic and bathymetric surveys. These STs were set where the river geometry showed important changes and near hydraulic structures. Geometrical information of the latter was retrieved from the structures final drawings and *in situ* measurements made for this purpose. Riverbed material was classified by local observations (Chow, 1959). Maximum flood levels in the Tavira urban area were obtained for the worst case scenario, *i.e.*, when the downstream-moving river flood wave overlaps the upstream-moving tide wave. This case scenario takes place when the river peak flow reaches the upstream boundary cross section 1 hour before the tidal high water occurs at the downstream boundary cross section.

4.3.3. Flood delimitation

The following cartographical data and the hydrodynamic model results were combined to define the 10- and 100-years recurrence period flood-affected areas:

- Portuguese Army topographical maps 1:25,000 and ortophotomaps;
- Topographical map of Tavira with contour lines every 10 m;
- Bathymetric survey of the Séqua/Gilão riverbed and the Tavira bar, Quatro Águas bar and Gilão River.

The flood-affected areas were delimited for the 10- and 100-years return period and the 100-years climate change scenario by retrieving, for each of the cross sections, the maximum flood levels from the hydrodynamic model. After completion of this process, the areas above the maximum flood which were within the flood delimitated area (island areas) were trimmed out.

4.3.4. Comparison of the model results with observed flood levels

In the night of the 3rd of December 1989 a severe flood occurred in Tavira with 120 mm of daily rainfall registered during that day at the São Brás de Alportel meteorological station.

Making use of an amateur video from that night and from flood level inscriptions still visible on some walls, some flood-affected locations were identified (Figure 9). Since it was possible to recognize from the video the maximum flood levels, by means of a set of *in-situ* measurements the depth of water in those locations was estimated (Table 10).

Location (point)	Observed flood depth (m)	Simulated flood depth (m)
A	2.5	2.9
C	4.4	4.3
D	4.4	4.3
H	2.7	3.1
K	4.1	4.1
M	4.4	4.3

Table 10. Comparison between the simulation results and the observed flood depths attained on the 3rd of December 1989 flood event.

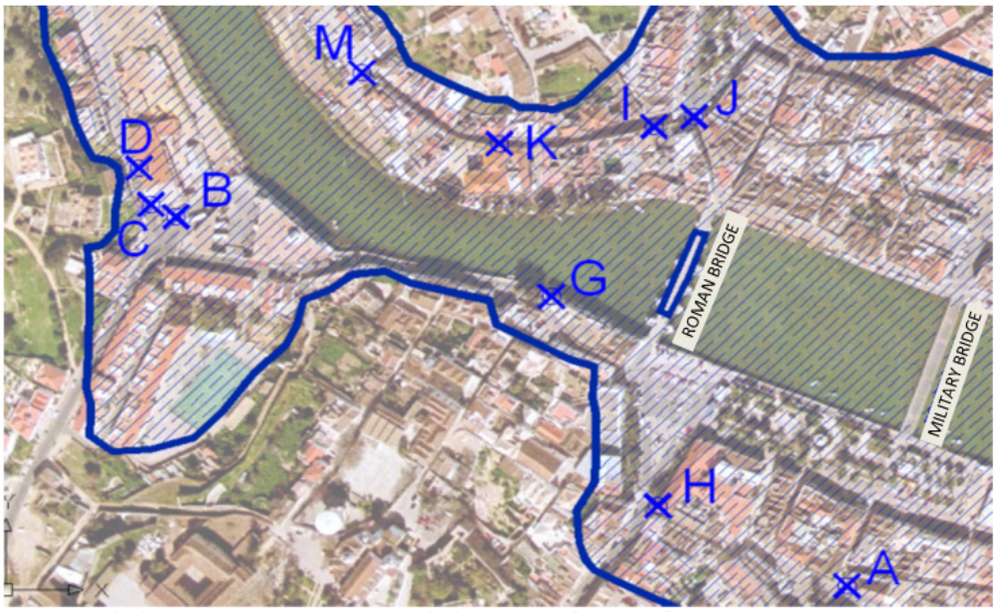

Figure 9. Location of places used to compare the simulation results and the observed flood depths attained on the 3rd of December 1989 flood event.

4.4. Results and discussion

The 10- and 100- year flood area maps of the Tavira urban area show that a significant part of the urban area which is adjacent to the Séqua/Gilão River is within the flood-affected perimeter (Figure 10). The City's centre is severely affected both by the simultaneous occurrence of high spring tide and the 10- or the 100-year rainfall events.

It is clearly visible that after the ST11 section the flood area expands widely. This is because ST11 represents a heritage bridge which causes significant obstruction to the river channel. A hydraulic gradient is formed by this bridge thus allowing water to overflow the river channel.

Figure 10. Flood delimitation for the Tavira urban area. Blue and magenta areas represent, respectively, the 10- and 100-years return period.

4.5. Conclusions

This application shows an example of how GIS-based soil data may be used as an input for flood-modelling purposes. In this example HEC-HMS (hydrological model) and HEC-RAS (hydraulic model) were used to obtain maximum flood levels for 10- and 100-years return periods.

5. General conclusions

This work aimed to illustrate how GIS-based models can be used as tools for environmental studies through three case studies in the south of mainland Portugal. The first dealt with the problem of geo-form classification in the Ria Formosa estuary. The second focused on using DEM/DTM-based climate models to obtain and analyze isohyetal maps and to identify rainfall distribution influence on water erosion at the Serra de Grândola. In the third application, GIS-based models were used to determine hydrological regional parameters for urban flood mapping purposes (this last application focused in the Séqua/Gilão River and the city of Tavira). The applications allowed demonstrating the versatility and usefulness of GIS-based models when used to solve environmental issues.

Author details

Jorge M. G. P. Isidoro
IMAR – Marine and Environmental Research Centre, Department of Civil Engineering, University of Algarve, Campus da Penha, Faro, Portugal

Helena M. N. P. V. Fernandez and Fernando M. G. Martins
Department of Civil Engineering, University of Algarve, Campus da Penha, Faro, Portugal

João L. M. P. de Lima
IMAR – Marine and Environmental Research Centre, Department of Civil Engineering, University of Coimbra, Rua Luís Reis Santos, Campus II – University of Coimbra, Coimbra, Portugal

Acknowledgement

This research was partly supported by project PTDC/ECM/105446/2008, funded by the Portuguese Foundation for Science and Technology (FCT) and by the Operational Programme "Thematic Factors of Competitiveness" (COMPETE) through the European Regional Development Fund (ERDF). The three first authors wish to acknowledge FCT Ph.D. grants SFRH/PROTEC/49736/2009, SFRH/PROTEC/67603/2010 and SFRH/PROTEC/67438/2010, respectively. The second and third authors also wish to express their gratitude to research group MED_Soil of the Department of Crystallography, Mineralogy and Agricultural Chemistry of the Faculty of Chemistry, University of Seville, Spain.

6. References

Anaya-Romero M, Pino R, Jordán A, Zavala LM, Bellinfante NC (2005). Modelización del hábitat potencial de formaciones forestales en la provincia de Huelva. *Edafología*, 12, 65-73 (in Spanish).

Anaya-Romero M, Jordán A, Zavala LM, Bellinfante NC (2004). A comparison of methods to predict the potential area of forest types in southern Spain, In: *Proceedings of the International Symposium on Forest Soils Under Global and Local Changes: From Research to Practice*, Institut Européen de la Forêt Cultivée, Bordeaux, September, 2004, pp. 119-120.

Arnoldus HM (1978). An aproximation of the rainfall factor in the Universal Soil Loss Equation, In: De Boodst M, Gabriels D, eds. *Assessments of erosion*, New York, John Wiley & Sons, Inc., pp. 127-132.

Bastian O (2000). Landscape classification in Saxony (Germany) - a tool for holistic regional planning. *Landscape and Urban Planning*, 50, pp. 145-155.

Bocco G, Mendoza M, Velázquez A (2001). Remote sensing and GIS-based regional geomorphological mapping—a tool for land use planning in developing countries. *Geomorphology*, 39, pp. 211-219.

Brunner GW (2008). *HEC-RAS River Analysis System – Hydraulic Reference Manual v. 4.0*. US Army Corps of Engineers – Hydrologic Engineering Center, Davis, CA, USA.

Burrough PA, Wilson JP, Van Gaans PFM, Hansen AJ (2001). Fuzzy k-means classification of topo-climatic data as an aid to forest mapping in the Greater Yellowstone Area, USA. *Landscape Ecology*, 16, pp. 523-546.

Cardoso J (1965). *Os Solos de Portugal, sua Classificação, Caracterização e Génese*, Direcção Geral dos Serviços Agrícolas, Lisbon (in Portuguese).

Cerdan O, Govers G, Le Bissonais Y, Van Oost K, Poesen J, Saby N, Gobin A, Vacca A, Quinton J, Auerswald K, Klik A, Kwaad F, Raclot D, Ionita I, Rejman J, Rousseva S, Muxart T, Roxo MJ, Dostal T. (2012). Rates and spatial variations of soil erosion in Europe: A study based on erosion plot data. *Geomorphology,* 122(1-2), pp. 167-177.

CORINE-CEC (1992). *CORINE soil erosion risk and important land resources. An assessment to evaluate and map the distribution of land quality and soil erosion risk*. Office for official publications of the European Communities, City of Luxemburg.

CORINE-CLC (2006). *Cartografia CORINE Land Cover 2006 para Portugal Continental*. Instituto Geográfico do Exército, Grupo de Detecção Remota, Lisbon (in Portuguese).

Chow VT (1959). *Open Channel Hydraulics*, New York, McGraw-Hill.

Chow VT, Mays L, Maidment D (1988). *Applied Hydrology,* New York, McGraw-Hill.

DGM (1984). *Carta Geológica à escala 1:50,000*. Direcção-Geral de Minas e Serviços Geológicos. Lisboa.

de Lima JLMP (2010) (ed.). *Hidrologia Urbana: Conceitos Básicos*. ERSAR - Entidade Reguladora de Serviços de Água e Resíduos, Lisbon (in Portuguese).

Díez-Herrero A, Gómez JL, Pérez IG, Azcárate JA, Moral SS, Jiménez JCC (2006). Análisis de la insolación directa potencial como factor de degradación de los conjuntos pictóricos rupestres de Villar del Humo (cuenca). *Proceedings of the IX Reunión Nacional de Geomorfología: Geomorfología y territorio*, Santiago de Compostela, 13-15 September 2006, pp. 903-1008 (in Spanish).

Dikau R (1989). The application of a digital relief model to landform analysis in geomorphology, In: Raper J, ed. *Three dimensional applications in Geographical Information Systems*, Taylor & Francis, London, pp. 51-77.

Dikau R, Brabb EE, Mark R (1991). *Landform classification of New Mexico by computer*. US Geological Survey, Open File Report 91/634.

Drãgut L, Blaschke T (2006). Automated Classification of Landform Elements Using Object-Based Image Analysis. *Geomorphology*, 81(3-4), pp. 330-344.

Eastman JR (2009). IDRISI Taiga, Worcester, Clark University.

Eswaran H, Reich P, Beinroth F (2001). Global desertification tension zones, In: Stott DE, Mohtar RH, Steinhardt GC, eds. 2001. *Sustaining the global farm. Selected papers from the 10th International Soil Conservation Organization Meeting*, 24-29 May 1999, Purdue, pp. 24-28.

FAO (1989). Role of forestry in combating desertification. *FAO Conservation Guide No. 21,* Forest Conservation and Wildlands Branch, Forest Resources Division, Forestry Department, Rome.

Favis-Mortlock DT, Guerra AJT (1999). The implications of general circulation model estimate of rainfall for future erosion: A case study from Brazil. *Catena*, 37, pp. 329-354.

Favis-Mortlock DT, Savabi MR (1996). Shifts in rates and spatial distributions of soil erosion and deposition under climate changes, In: Anderson MG, Brooks SM, eds. *Advances in Hillslope Processes*, Vol. 1, Chichester, Wiley.

Felicísimo AM (1999). La utilización de los MDT en los estudios del medio físico. *150 aniversario de la creación del Instituto Tecnológico Geominero de España*, Universidad de Oviedo, Oviedo (in Spanish).

Feng X, Wang Y, Chen L, Fu B, Bai G (2010). Modelling soil erosion and its response to land-use changes in hilly catchments of the Chinese Loess Plateau. *Geomorphology*, 118, pp. 239-248.

Fernandez HM (2004). *Aplicação da Geostatística na Criação de um Modelo Digital de Terreno* (MSc Thesis). Technical University of Lisbon, Lisbon (in Portuguese).

Flanagan DC, Renschler CS, Cochrane TA (2000). Application of the WEPP model with digital topographic information, In: Parks BO, Clarke KM, Crane MP, eds. *Proceedings of the 4th International Conference on Integrating Geographic Information Systems and Environmental Modeling: Problems, Prospectus, and Needs for Research*, Banff, September, 2000.

Fournier F (1960). *Climat et érosion*. Paris, Presses Universitaires de France (in French).

Gerçerk D, Toprak V, Strobl J (2011). Object-based classification of landforms based on their local geometry and geomorphometric context. *International Journal of Geographical Information Science*, 25 (6), pp. 1011-1023.

Gonçalves MC, Ramos TB, Martins JC, Kosmas C (2010). Use of PESERA and MEDALUS models to assess soil erosion risks and land desertification in Vale do Gaio watershed. *Revista de Ciências Agrárias*, 33(1), pp. 236-246.

Guo JC (2006). *Urban Hydrology and Hydraulic Design*. Water Resources Publication, ISBN-13 978-1-887201-48-3, ISBN-10 1-887201-48-3, Highlands Ranch, CO.

Hammond EH (1954). Small scale continental landform maps. *Annals of the Association of American Geographers*, 44, pp. 34-42.

Hammond EH (1964). Classes of landsurface form in the forty-eight states, USA. *Annals of the Association of American Geographers*, Map Supplement No. 54.

Herrington L, Pellegrini G (2000). An advanced shape of country classifier: extraction of surface features from DEMs., In: Parks BO, Clarke KM, Crane MP, eds. *Proceedings of the 4th International Conference on Integrating Geographic Information Systems and Environmental Modeling: Problems, Prospectus, and Needs for Research*, Banff, September, 2000.

IGeoE (2004). *Carta Militar de Portugal à escala 1:25000*. Instituto Geográfico do Exército, Lisbon (in Portuguese).

Jordán A, Zavala LM, Bellinfante NC, González-Peñaloza FA (2005). Cartografía semicuantitativa del riesgo de erosión en suelos mediterráneos, In: Jiménez-Ballesta, R, ed., *Proceedings of the II Simposio Nacional sobre Control de la Degradación de Suelos*, Madrid, July, 2005, pp. 701-706 (in Spanish).

Jordán A, Zavala LM, Anaya-Romero M, Bellinfante NC (2007a). Propuesta de un Modelo de Distribución de Especies Forestales en el parque Natural Sierra de Aracena y el Andévalo Occidental (Huelva, España), In: Bellinfante NC, Jordán A, eds. *Tendencias Actuales de la Ciencia del Suelo*, Universidad de Sevilla, Seville, pp. 993-1002 (in Spanish).

Jordán A, Zavala LM, Peñaloza FG, Bellinfante NC (2007b). Elaboración de un modelo de geoformas del terreno, In: Bellinfante NC, Jordán A, eds. *Tendencias Actuales de la Ciencia del Suelo*, Universidad de Sevilla. Seville. pp. 792-803 (in Spanish).

Koop E, Sobral M, Soares T, Woerner M (1989). *Os Solos do Algarve e Suas Características*, Direcção Regional de Agricultura do Algarve, Faro (in Portuguese).

Kosmas C, Danalatos NG, Gerontidis S. (2000). The effect of land parameters on vegetation performance and degree of erosion under Mediterranean conditions. *Catena*, 40, pp. 3-17.

Lencastre A, Franco FM (1992). *Lições de Hidrologia,* Monte da Caparica, Universidade Nova de Lisboa (in Portuguese).

Lillesand TM, Kiefer RW, Chipman JW (2004). *Remote Sensing and Image Interpretation* (5th edition), New York, John Wiley and Sons Inc.

MacMillan RA, Pettapiece WW, Nolan SC, Goddard TW (2000). A generic procedure for automatically segmenting landforms into landform elements using DEMs, heuristic rules and fuzzy logic. *Fuzzy Sets and Systems*, 113, 81–109.

Maidment DR (ed.) (2000). *ArcGIS Hydro data model: Draft data model and manuscript, Proceedings of the GIS Hydro 2000*. San Diego, June 2000.

Oliveira AM, Santos RL (2009). Análise comparativa entre fatiamento e a classificação de imagens aplicada ao mapeamento das unidades de vertentes em Feira de Santana-BA. *Proceedings of the XIII Simpósio Brasileiro de Geografia Física Aplicada*, Universidade Federal de Viçosa, Viçosa, Julho, 2009 (in Portuguese).

PAP/RAC (1997). *Guidelines for mapping and measurement of rainfall-induced erosion processes in the Mediterranean coastal areas*, Split, UNEP/FAO.

Pimentel D (2006). Soil erosion: a food and environmental threat. *Environment, Development and Sustainability*, 8, pp. 119-137.

Pino R, Anaya-Romero M, Cubiles de la Vega MD, Pascual Acosta A, Jordán A, Bellinfante NC (2010). Predicting the potential habitat of oaks with data mining models and the R system. *Environmental Modelling & Software*, 25, pp. 826-836

Prasad T (1997). GIS Applications for Flood Simulation and Management, In: Misra B, ed. *Geographic Information System and Economic Development: Conceptual Applications*, New Delhi, Mittal Publications, pp. 49–56.

Pruski FF, Nearing MA (2002). Climate-induced changes in erosion during the 21st. century for eight U.S. locations. *Water Resources Research*, 38(12), pp. 1298-1308.

Rouse JW, Hass RH, Schell JA, Deering DW (1974). *Monitoring the vernal advancement and retrogradation (Greenwave effect) of nature vegetation*, NASA/GSFCT Type III Final Report, Greenbelt.

Sallun AEM, Suguio K, Filho WS (2007). Geoprocessing for Alto Rio Paraná Allogroup Cartography (SP, PR e MS). *Revista Brasileira de Cartografia*, 59, pp. 289-299.

SROA (1970). *Carta de Solos de Portugal*. Secretaria de Estado da Agricultura, Lisbon.

StatSoft, Ltd (2001). *STATISTICA (data analysis software system), v.6 users manual*, Statsoft Inc. Tulsa.

Teng Z, Xuezhi C, Ruoyin L, Guoan T (2009). Landform classification based on hillslope units from DEMs. *Proceedings of the 30th Asian Conference on Remote Sensing,* Beijing, October, 2009.

Umbelino G, Carvalho R, Antunes A (2009). Uso da Cartografia Histórica e do SIG para a reconstituição dos caminhos da Estrada Real. *Revista Brasileira de Cartografia,* 61(1), pp. 63-70 (in Portuguese).

Williams J, Nearing MA, Nicks A, Skidmore E, Valentine C, King K, Savabi R (1996). Using soil erosion models for global change studies. *Journal of Soil and Water Conservation*, 51 (5), pp. 381-385.

Wooldridge SA, Kalma JD (2001). Regional-scale hydrological modelling using multiple-parameter landscape zones and a quasi-distributed water balance model. *Hydrology and Earth System Sciences*, 5(1), pp. 59–74.

Yang D, Kannae S, Oki T, Koike T, Musiake K (2003). Global potencial soil erosion with reference to land use and climate changes. *Hidrological Processes*, 17(14), pp. 2913-2928.

Zavala LM, Jordán A, Anaya-Romero M, Bellinfante NC (2004). Cartografía semicuantitativa del riesgo de erosión hídrica. *Edafología*, 12, pp. 79-87 (in Spanish).

Zavala LM, Jordán A, Anaya-Romero M, Gómez IA, Bellinfante NC (2005a). Clasificación automática de elementos geomorfológicos en la cuenca del Río Tepalcatepec (México) a partir de un modelo digital de elevaciones: Clasificación automática de formas del terreno. *Cuaternario y Geomorfologia*, 19, pp. 49-61 (in Spanish).

Zavala LM (2001). Análisis territorial de la comarca del Andévalo Occidental: Una aproximación desde el medio físico (PhD Thesis). University of Seville, Seville (in Spanish).

Zavala LM, Jordán A, Illana P (2007). Aplicación de un sistema de información geográfica al análisis del medio físico en el Parque Natural Los Alcornocales: Aproximación a una cartografía geomorfológica a partir de un modelo digital de elevaciones, *Almoraima*, 35, pp. 245-254 (in Spanish).

Zavala LM, Jordán A, Gómez IA, Anaya-Romero M, Girón V, Segura D (2005b). Estudio del riesgo de erosión potencial en la cuenca alta del Río Hozgarganta. *Almoraima*, 31, pp. 111-118 (in Spanish).